A Journal of the Gesellschaft Deutscher Chemiker

Angewandte International Edition GDCh Chemie

www.angewandte.org

Accepted Article

Title: A Double-Walled Tetrahedron with AgI4 Vertices Binds Different Guests in Distinct Sites

Authors: Samuel Edward Clark, Andrew W. Heard, Charlie T. McTernan, Tanya K. Ronson, Barbara Rossi, Petr Rozhin, Silvia Marchesan, and Jonathan Russell Nitschke

To be cited as: *Angew. Chem. Int. Ed.* **2023**, e202301612

Link to VoR: https://doi.org/10.1002/anie.202301612

WILEY-VCH

10.1002/anie.202301612

WILEY-VCH

COMMUNICATION

A Double-Walled Tetrahedron with Ag^{I}_{4} Vertices Binds Different Guests in Distinct Sites

Samuel E. Clark,[a] Andrew W. Heard,[a, b] Charlie T. McTernan,[a, c, d] Tanya K. Ronson,[a] Barbara Rossi,[e] Petr Rozhin,[f] Silvia Marchesan*[f], and Jonathan R. Nitschke*[a]

[a] S. E. Clark, Dr A. W. Heard, Dr C. T. McTernan, Dr T. K. Ronson, Prof J. R. Nitschke
Yusuf Hamied Department of Chemistry
University of Cambridge
Lensfield Road, Cambridge, CB2 1EW, U.K.
E-mail: jrn34@cam.ac.uk
[b] Dr A. W. Heard
Astex Pharmaceuticals
436 Cambridge Science Park, Milton Road, Cambridge, CB4 0QA, U.K.
[c] Dr C. T. McTernan
The Francis Crick Institute
Midland Road, London, NW1 1AT, U.K.
[d] Dr C. T. McTernan
Department of Chemistry
King's College London
7 Trinity Street, London, SE1 1DB, U.K.
[e] Dr B. Rossi
Elletra Sincrotrone Trieste
Basovizza, Trieste, IT-34149, Italy
[f] P. Rozhin, Prof S. Marchesan
Department of Chemical and Pharmaceutical Science
University of Trieste
Trieste, IT-34127, Italy
E-mail: smarchesan@units.it

Supporting information for this article is given via a link at the end of the document.

Abstract: A double-walled tetrahedral metal-organic cage assembled in solution from silver(I), 2-formyl-1,8-naphthyridine, halide, and a threefold-symmetric triamine. The $Ag^{I}_{4}X$ clusters at its vertices bring together six naphthyridine-imine moieties, leading to a structure in which eight tritopic ligands bridge four clusters in an $(Ag^{I}_{4}X)_4L_8$ arrangement. Four ligands form an inner set of tetrahedron walls that are surrounded by the outer four. The cage has significant interior volume, and was observed to bind anionic guests. The structure also possesses external binding clefts, located at the edges of the cage, which bound small aromatic guests. Halide ions bound to the silver clusters were observed to exchange in a well-defined hierarchy, allowing modulation of the cavity volume. The principles uncovered here may allow for increasingly more sophisticated cages with silver-cluster vertex architectures, with post-assembly tuning of the interior cavity volume enabling targeted binding behavior.

Metal-organic cages that assemble from metal ions and organic ligands possess well-defined interior cavities that can bind guests selectively. These molecular containers have applications in molecular recognition and chemical separations,[1] stabilization of highly reactive molecules,[2] catalysis,[3] and sensing.[4] Subcomponent self-assembly, whereby higher-order cage structures emerge from simple precursors through the simultaneous formation of covalent C=N and coordinative N→metal coordination bonds, has allowed others[3d,5] and our group[1f,6] to prepare intricate three-dimensional structures, encompassing Platonic and Archimedean solids, and beyond.[7] Different design strategies produce architectures with different sizes and symmetries,[8] allowing tuning of the interior cavity's sizes and properties.

The potential utility of Ag^{I} as a structural metal ion in such complex cages is highlighted by an elegant series of topologically entangled cages bound with silver(I) reported by Fujita and co-workers,[9] as well as a range of Ag^{I}-carbene cages and metallacycles.[10] The flexible coordination environment of Ag^{I} has also been used to synthesize a range of Ag^{I}-dipyridylpeptide coordination complexes, achieving even greater topological complexity.[11]

Self-assembled metal-organic structures that incorporate polymetallic clusters as vertices,[12] as opposed to single metal ions, are beginning to be developed.[13] Strategies that enable the rational design of these more intricate assemblies are likewise under investigation. The ability of the 'soft' metal Ag^{I} to form clusters[14] and to support differing coordination numbers and environments makes this metal well suited to the formation of cluster-vertex assemblies.[15] We have reported a trigonal-prismatic structure containing disilver vertices,[16] and a series of hexameric helicates containing tetra- and hexa-silver clusters as vertices.[17] These structures demonstrate the diverse co-ordination environments that emerge when naphthyridine-imine ligands direct the formation of Ag^{I} clusters. However, previous structures provided relatively small internal volumes for guest binding.

In this work, we report the incorporation of $[Ag^{I}_{4}I]^{3+}$ clusters into a previously unreported type of double-walled tetrahedral structure,[18] and explore its guest binding potential. This structure exhibits both interior and peripheral guest binding, with distinct groups of guests favoring each site. Furthermore, we found that the silver clusters at the tetrahedron vertices underwent halide exchange, which enabled us to finely tune the volume of the interior cavity.

10.1002/anie.202301612

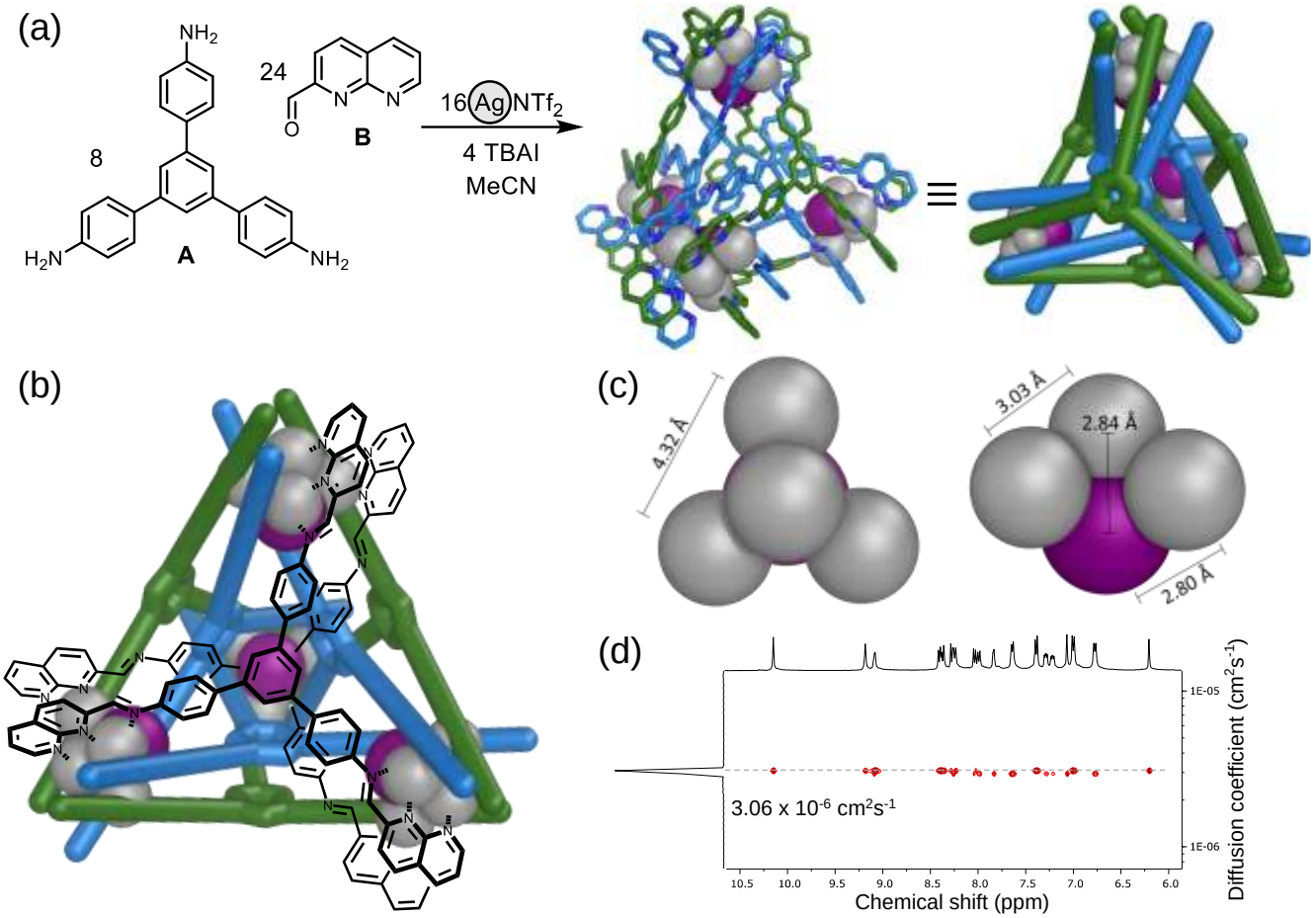

Figure 1. (a) Self-assembly of subcomponents **A** and **B** with $Ag^{I}NTf_2$ and TBAI, forming double-walled $[Ag^{I}_{16}I_4\mathbf{L}_8](NTf_2)_{12}$ tetrahedron **1**, showing two representations of the X-ray crystal structure of the cationic part of **1**. (b) Coordination of ligand **L** in the inner and outer face, with other ligands shown as cartoon representations. (c) Detailed view of the structure of the $[Ag^{I}_4I]^{3+}$ cluster, with A···Ag and Ag···I distances marked in Angstroms (Å). (d) ^{1}H DOSY NMR spectra of **1**.

The reaction between 1,3,5-tris(4-aminophenyl)benzene (**A**, 8 equiv.) with 2-formyl-1,8-naphthyridine (**B**, 24 equiv.), Ag^{I} bis(trifluoromethanesulfonyl)imide (triflimide or -NTf_2, 16 equiv.) and tetra-*n*-butylammonium iodide (TBAI, 4 equiv.) produced cage **1** (Figure 1a). The ^{1}H nuclear magnetic resonance (NMR) spectra of **1** exhibited two magnetically distinct ligand environments (Figure 1b), with two distinct imine signals assigned by heteronuclear single quantum coherence spectroscopy (HSQC) (Figure S6). The diffusion ordered spectroscopy (DOSY) NMR spectrum confirmed that both environments corresponded to a single discrete structure, with a diffusion coefficient of 3.06 × 10^{-6} cm^2s^{-1} in CD_3CN, giving a solvodynamic radius of 21.2 Å (Figure 1d). The mass spectrum (Figure S10–14) indicated a $[Ag_{16}I_4\mathbf{L}_8]^{12+}$ composition.

Single-crystal X-ray diffraction revealed the molecular structure of **1** to be a *T*-symmetric double-walled tetrahedron.[19] Two tritopic ligands span each face of the tetrahedron (Figure 1a), consistent with NMR and mass spectrometry. Each vertex consists of a $[Ag_4I]^{3+}$ cluster (Figure 1c), with Ag^{I}···Ag^{I} distances of 3.03 Å between the capping Ag^{I} and each of the three Ag^{I} centers closer to iodide. This distance is within the sum of the Van de Waals radii (3.44 Å) for two Ag^{I} ions, and similar to the 2.97–3.00 Å distance reported for previous vertex clusters[17] and other naphthyridine-bridged Ag^{I} clusters.[20] The phenyl core of the inner and outer ligands is separated by 3.67 Å, in the typical range for a π-π stacking interaction. The structure has a distance between farthest-spaced silver ions of 18.7 Å, comparable to the solvodynamic radius observed in DOSY. The innermost triads of Ag^{I} ions were separated by 4.32 Å, suggesting that these Ag^{I} ions do not undergo argentophilic interactions with each other.

Three observations help clarify how the naphthyridine-imine ligand binding groups help shape the silver clusters at the vertices of **1**. First, the imine nitrogen atoms of the inner panels (blue in Figure 1) are oriented away from the Ag^{I} centers, and are therefore uncoordinated. Second, the outer ligands (green in Figure 1) adopt a bridging role, with each naphthyridine N-atom bound to a different Ag^{I} center (Figure 1b). Third, in contrast with these outer-ligand naphthyridines, one in each pair of naphthyridine N-atoms of the inner (blue) ligands effectively chelates Ag^{I} ions from the inner set closest to iodide. Each inner Ag^{I} thus coordinates to one naphthyridine nitrogen from an inner (blue) ligand and one from an outer (green) ligand. The flexibility of naphthyridine to either bridge or chelate Ag^{I} thus appears to again play an important role in bringing the silver-cluster vertices of **1** together, as has been observed elsewhere.[16,17,21]

The tight arrangement of tritopic ligands around the cage interior results in a high degree of enclosure. The available cavity space within **1** was calculated to be 103 $Å^3$ using Molovol.[22] With this available volume in mind, small neutral and anionic species were screened as potential guests for **1**.

10.1002/anie.202301612

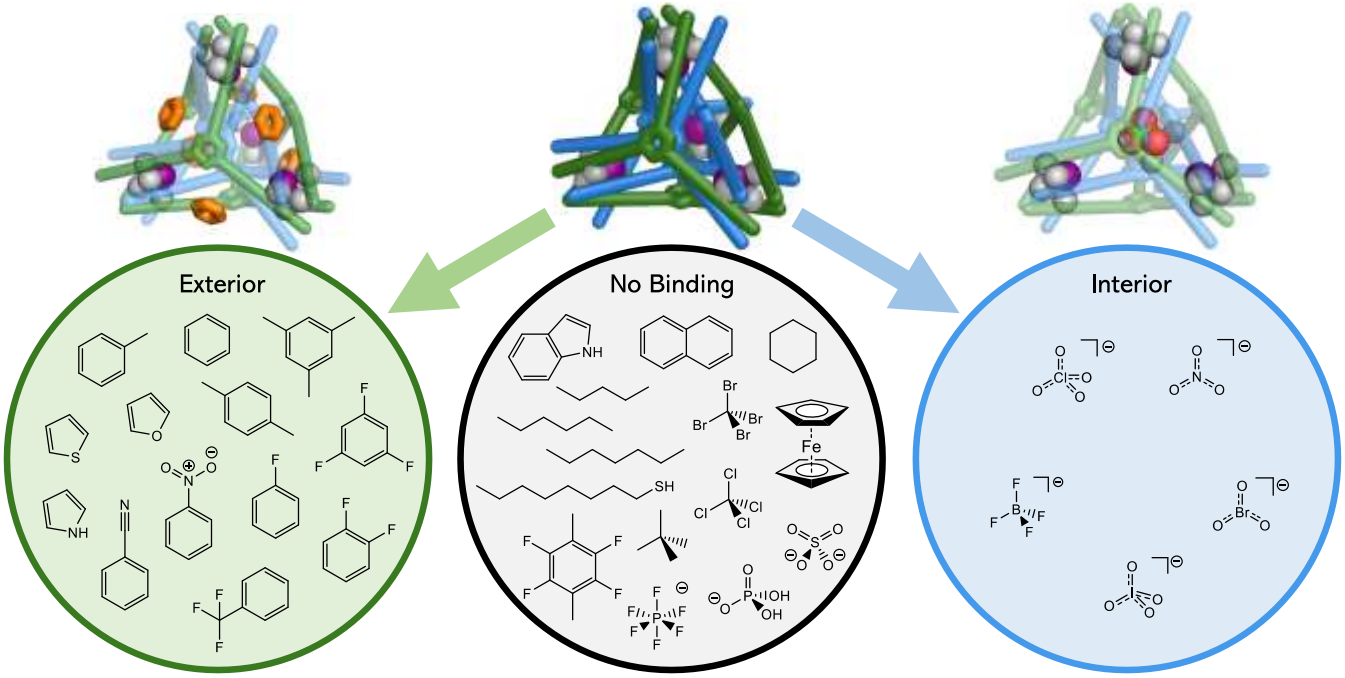

Figure 2. Schematic depicting the exterior (left) and interior (right) binding modes of double-walled tetrahedron **1**. Anionic guests bound within **1** are depicted in the blue circle at right. Small aromatic guests bound at the exterior of **1** are shown in the green circle at left. No binding was observed for the molecules shown in the central (black) circle. BrO_3^- was introduced as the potassium salt; all other anionic guests were used as the tetra-*n*-butylammonium salts.

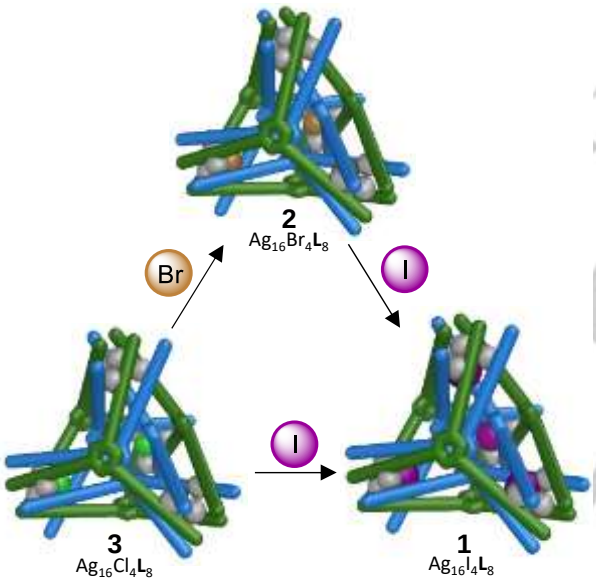

Figure 3. Successive halide exchange at the Ag^I_4 clusters resulted in sequential transformations, allowing us to assign silver cluster halide affinity in the order I^- > Br^- > Cl^-. Halides were added as the tetra-*n*-butylammonium salts. See Supporting Information, Figure S43-48 for ^{1}H NMR data.

In many cases, no change was observed in the NMR spectrum (Figure 2) upon adding the prospective guest to host **1**. The addition of anionic guests nitrate (NO_3^-), periodate (IO_4^-), bromate (BrO_3^-), tetrafluoroborate (BF_4^-), and perchlorate (ClO_4^-) led to ^{1}H NMR shifts of 0.04–0.10 ppm for the inward-facing imine ^{1}H signal, with no shift observed for externally-oriented imine (see SI, Section 8). This observation supports the assignment of interior binding (K_a = *2*–9 × 10^2 M^{-1}, see Supporting Information Table S4), taking place in fast exchange on the NMR time scale. The volume of the anionic guests lay in the range 41.1–67.7 Å^3; all guests are of appropriate volume for the measured cavity volume of **1**. Binding occurs with a 1:1 stoichiometry, as supported by a Job plot (Figure S67), and we infer binding to be driven by coulombic interactions between the guests and the cationic Ag^I ions of the cage framework.

Small aromatic molecules were observed to bind externally to **1**. The presence of these guests (Figure 2) resulted in shifts to NMR signals of **1** assigned to externally-oriented hydrogen atoms, as opposed to the internal ones observed to shift for anionic guests. For these prospective guests, binding was inferred to have taken place when chemical shifts changed by at least 0.04 ppm upon guest addition. A 2D rotating-frame nuclear Overhauser effect correlation spectroscopy (ROESY) NMR spectrum showed correlations between added benzene and ^{1}H NMR signals assigned to the tetrahedron edges (Figure S57), supporting the hypothesis that benzene binds at these sites. We thus infer that binding occurs externally with binding affinities of approximately 2 × 10^2 M^{-1} (Supporting Information Table S4), involving aromatic stacking and van der Waals interactions between the guest and the large aromatic surface area exposed on the exterior six edges of the tetrahedron cage **1**. A Job plot showed a clear maximum at a molar fraction of benzene at 0.85, supporting a 6:1 binding stoichiometry (Figure S66).[23] The assignment of this binding mode is further supported by the lack of NMR changes observed for larger aromatics, such as naphthalene.

For many of the potential guests trialed, no evidence of binding was observed. We infer that non-planar, uncharged guests, such as hexane, tetrabromomethane, and neopentane do not engage in the aromatic stacking interactions of the exterior binding mode, nor do they benefit from an electrostatic driving force for encapsulation in the interior cavity. The presence of larger aromatic guests also caused no change in NMR spectra. We attribute this observation to the guest being too large for the external binding cleft. Three charged guests were also observed

not to bind. In the case of PF_6^-, the guest is significantly larger than other interior binding guests, thus likely exceeding the upper limit for interior binding. In the other two cases (SO_4^{2-} and $H_2PO_4^-$) addition of the guest instead led to degradation of the cage.

Synthesis of **1** was repeated using other halides, as TBAF, TBACl and TBABr, in place of TBAI. While fluoride did not lead to clean assembly, the formation of analogs of **1** were observed with bromide (**2**) and chloride (**3**) as templating ions. The DOSY NMR confirmed the formation of a similarly sized species, with two distinct ligand environments in the ^{1}H NMR spectrum. Mass spectrometry confirmed the presence of the $[Ag_{16}X_4L_8](NTf_2)_{12}$ species in solution.

We hypothesized that stronger binding between iodide and Ag^I could provide a driving force for halide exchange within the silver cluster. Such exchanges were observed to proceed, with a binding hierarchy of $I^- > Br^- > Cl^-$, shown in Figure 3. These processes were monitored by ^{1}H NMR spectroscopy (Figures S43–48). These NMR spectra indicated the presence of intermediate species that incorporated two different halides, in slow exchange on the NMR time scale. Broadening of the ^{1}H NMR spectra was observed alongside halide addition both in the case of halide exchange and excess of a lighter halide, attributed to possible aggregation or interior halide binding.

Numerous attempts did not result in the isolation of single crystals of **2** or **3** with sufficient quality for X-ray analysis. However, modeling using the Scigress extended-MM3 method[24] with the crystal structure of **1** as a starting point allowed estimation of the differences in interior volume.[25] Analyses of the interiors in the modeled structures of cages **2** and **3** using Molovol[22] gave cavity volumes of 111 Å^3 and 113 Å^3 respectively.

Raman spectroscopy was used to verify the structure of cages **1–3** in thin films and in solution. Visible-light Raman spectra of thin films of cages **1–3** were dominated by signals arising from aromatic ligand coordination to the metal centers in the region 1550–1650 cm^{-1}.[26] Aniline signals were not observed, confirming the absence of cage hydrolysis (Figure S39). Evidence was observed for the presence of silver clusters in the region below 500 cm^{-1} (Figure S40). The Ag···Ag distance of 2.94 Å between the basal and apical Ag^I centers, obtained from the crystal structure of **1**, was used in conjunction with Herschbach–Laurie relationships[27] as implemented by Harvey *et al*.[28] From this relationship, a predicted Ag···Ag force constant of 0.236 mdyn Å^{-1} was obtained, which corresponds to a stretching frequency of 86 cm^{-1} (see Supporting Information page S35). Force constants determined this way have previously shown good agreement with experimentally determined Raman shifts.[27] While we were not able to observe the Ag···Ag stretching band directly due to instrumental limits of Rayleigh rejection, the fundamental frequency was confirmed by two overtone peaks at 323 cm^{-1} and 409 cm^{-1}, with the corresponding spacing ($\Delta\nu$ = 86 cm^{-1}) as previously reported for Ag clusters.[29]

Similar results were obtained for thin films of cages **2** and **3** (319–320 cm^{-1}, 409 cm^{-1}, Figure S40), corresponding to overtones of a fundamental stretching band at 89–90 cm^{-1}. This corresponds to a Ag···Ag force constant of ~0.25 mdyn Å^{-1}, with a shorter Ag···Ag distance consistent with Ag-Br and Ag-Cl bonding being weaker relative to Ag-I, and the atomic radii of Br and Cl being smaller than for I. These observations support our hypothesis that the cage framework remains unchanged upon substitution of the halide. Importantly, solution-state ultraviolet (UV) Resonance Raman measurements, performed at the Elettra synchrotron radiation facility using deep-UV excitation wavelength (λ = 266 nm, Figure S41) close to the resonance of the aromatic moieties, resulted in the appearance of two signals at 1587 and 1603 cm^{-1}, likely resulting from non-covalent interactions between the double walls of the cage.

These Raman measurements thus provided evidence to support three conclusions. Firstly, that the double-walled cage framework persists in both the solid and solution states. Secondly, that subtle differences in Ag···Ag stretching overtones report the presence of the different halides. Thirdly, that the ligands comprising the double walls of the cage are more mobile in solution than in the solid state. Absence of aniline peaks also confirmed cage integrity in solution. In the future, this spectroscopic approach may be useful for the structural characterization of cages for which single-crystal X-ray structure data is not available.

The structures of **1–3** thus make a significant addition to the small set of known double-walled container molecules,[18,30] with the added unusual property of having identical ligands occupying both interior and exterior faces and the ability to bind guests in two distinct environments. The assembly of **1–3** was enabled by the remarkable ability of naphthyridine-imine ligands to support and shape silver(I) clusters. Analogous structures with extended ligands and thus the capacity to enclose larger guests may enable the design of chemical sensors, where luminescent silver cluster vertices[31] report on guest presence and identity.

Acknowledgements

We thank Diamond Light Source (UK) for synchrotron beamtime on I19 (CY21497). S.E.C is the recipient of a PhD Studentship from BP through the BP International Centre for Advanced Materials (bp-ICAM). A.W.H. is the recipient of an Astex Pharmaceuticals Sustaining Innovation Post-Doctoral Award. C.T.M. thanks the Leverhulme Trust, the Isaac Newton Trust, and Sidney Sussex College, Cambridge, for financial support. We acknowledge Elettra Sincrotrone Trieste for providing access to its synchrotron radiation facilities (proposal number 20220534) and networking support from COST Action CA17139 (eutopia.unitn.eu) funded by COST (www.cost.eu).

Keywords: Metal-Organic Cages • Supramolecular Chemistry • Self-assembly • Metal Clusters

[1] a) W. M. Bloch, Y. Abe, J. J. Holstein, C. M. Wandtke, B. Dittrich, G. H. Clever, *J. Am. Chem. Soc.* **2016**, *138*, 13750–13755.; b) Z. Zhang, D. S. Kim, C.-Y. Lin, H. Zhang, A. D. Lammer, V. M. Lynch, I. Popov, O. Š. Miljanić, E. V. Anslyn, J. L. Sessler, *J. Am. Chem. Soc.* **2015**, *137*, 7769–7774; c) H. L. Ozores, M. Amorín, J. R. Granja, *J. Am. Chem. Soc.* **2017**, *139*, 776–784; d) R. Custelcean, P. V. Bonnesen, N. C. Duncan, X. Zhang, L. A. Watson, G. Van Berkel, W. B. Parson, B. P. Hay, *J. Am. Chem. Soc.* **2012**, *134*, 8525–8534; e) M. Yamashina, Y. Tanaka, R. Lavendomme, T. K. Ronson, M. Pittelkow, J. R. Nitschke, *Nature* **2019**, *574*, 511–515; f) D. Zhang, T. K. Ronson, Y.-Q. Zou, J. R. Nitschke, *Nat. Rev. Chem.* **2021**, *5*, 168–182; g) C. J. Bruns, D. Fujita, M. Hoshino, S. Sato, J. F. Stoddart, M. Fujita, *J. Am. Chem. Soc.* **2014**, *136*, 12027–12034; h) C. Fuertes-Espinosa, J. Murillo, M. E. Soto, M. R. Ceron, R. Morales-Martínez, A. Rodríguez-Fortea, J. M. Poblet, L. Echegoyen, X. Ribas, *Nanoscale* **2019**, *11*, 23035–23041; i) S. Fang, W.

Sun, C. Lin, F. Huang, H. Li, *Inorg. Chem.* **2023**, *62*, 1776-1780; j) Q. Li, Y. Wu, J. Cao, Y. Liu, Z. Wang, H. Zhu, H. Zhang, F. Huang, *Angew. Chem. Int. Ed.* **2022**, *61*, e202202381; k) A. Fuertes, M. Amorín, J. R. Granja, *Chem. Commun.* **2020**, *56*, 46–49; l) J.-L. Zhu, D. Zhang, T. K. Ronson, W. Wang, L. Xu, H.-B. Yang, J. R. Nitschke, *Angew. Chem. Int. Ed.* **2021**, *60* (21), 11789-11792.

[2] P. Mal, B. Breiner, K. Rissanen, J. R. Nitschke, *Science* **2009**, *324*, 1697–1699.

[3] a) M. Yoshizawa, M. Tamura, M. Fujita, *Science* **2006**, *312*, 251–254; b) C. M. Hong, R. G. Bergman, K. N. Raymond, F. D. Toste, *Acc. Chem. Res.* **2018**, *51*, 2447–2455; c) D. M. Kaphan, M. D. Levin, R. G. Bergman, K. N. Raymond, F. D. Toste, *Science* **2015**, *350*, 1235–1238; d) W. Cullen, M. C. Misuraca, C. A. Hunter, N. H. Williams, M. D. Ward, *Nat. Chem.* **2016**, *8*, 231–236; e) P. Howlader, P. Das, E. Zangrando, P. S. Mukherjee, *J. Am. Chem. Soc.* **2016**, *138*, 1668–1676; f) Y. Fang, J. A. Powell, E. Li, Q. Wang, Z. Perry, A. Kirchon, X. Yang, Z. Xiao, C. Zhu, L. Zhang, F. Huang, H. C. Zhou, *Chem. Soc. Rev.* **2019**, *48*, 4707–4730; g) D. Chu, W. Gong, H. Jiang, X. Tang, Y. Cui, Y. Liu, *CCS Chem.* **2022**, *4*, 1180–1189; h) F. F. Chu, L.-J. Chen, S. Chen, G.-Y. Wu, W.-L. Jiang, J.-C. Shen, Y. Qin, L. Xu, H.-B. Yang, *Chem* **2020**, *6*, 2395-2406; i) E. Ubasart, O. Borodin, C. Fuertes-Espinosa, Y. xu, C. García-Simón, L. Gómez, J. Juanhuix, F. Gándara, I. Imaz, D. Maspoch, M. von Delius, X. Ribas, *Nat. Chem.* **2021**, *13*, 420-427; j) J Jökel, F. Schwer, M. von Delius, U.-P. Apfel, *Chem. Comm.* **2020**, *56*, 14179-14182.

[4] a) K. Wu, K. Li, Y.-J. Hou, M. Pan, L.-Y. Zhang, L. Chen, C.-Y. Su, *Nat. Commun.* **2016**, *7*, 10487; b) W. Xue, T. K. Ronson, Z. Lu, J. R. Nitschke, *J. Am. Chem. Soc.* **2022**, *144*, 6136–6142; c) M. Denis, L. Qin, P. Turner, K. A. Jolliffe, S. M. Goldup, *Angew. Chem. Int. Ed.* **2018**, *57*, 5315–5319; d) M. Denis, J. Pancholi, K. Jobe, M. Watkinson, S. M. Goldup, *Angew. Chem. Int. Ed.* **2018**, *57*, 5310–5314; e) J. Pancholi, D. J. Hodson, K. Jobe, G. A. Rutter, S. M. Goldup, M. Watkinson, *Chem. Sci.* **2014**, *5*, 3528–3535; f) K. Jobe, C. H. Brennan, M. Motevalli, S. M. Goldup, M. Watkinson, *Chem. Commun.* **2011**, *47*, 6036.

[5] a) R.-J. Li, A. Tarzia, V. Posligua, K. E. Jelfs, N. Sanchez, A. Marcus, A. Baksi, G. H. Clever, F. Fadaei-Tirani, K. Severin, *Chem. Sci.* **2022**, *13*, 11912–11917; b) W. Li, C. Liu, J. Kfoury, J. Oláh, K. Robeyns, M. L. Singleton, S. Demeshko, F. Meyer, Y. Garcia, *Chem. Commun.* **2022**, *58*, 11653–11656; c) Y. Lei, Q. Chen, P. Liu, L. Wang, H. Wang, B. Li, X. Lu, Z. Chen, Y. Pan, F. Huang, H. Li, *Angew. Chem. Int. Ed.* **2021**, *60*, 4705–4711.

[6] a) C. T. McTernan, J. A. Davies, J. R. Nitschke, *Chem. Rev.* **2022**, *122*, 10393–10437; b) D. Zhang, T. K. Ronson, J. R. Nitschke, *Acc. Chem. Res.* **2018**, *51*, 2423–2436.

[7] a) J. P. Carpenter, C. T. McTernan, J. L. Greenfield, R. Lavendomme, T. K. Ronson, J. R. Nitschke, *Chem* **2021**, *7*, 1534–1543; b) J. A. Davies, T. K. Ronson, J. R. Nitschke, *Chem* **2022**, *8*, 1099–1106; c) T. K. Ronson, Y. Wang, K. Baldridge, J. S. Siegel, J. R. Nitschke, *J. Am. Chem. Soc.* **2020**, *142*, 10267–10272; d) L. Xu, Y.-X. Wang, L.-J. Chen, H.-B. Yang, *Chem. Soc. Rev.* **2015**, 44, 2148-2167; e) Z. Liu, Z. Tian, W. Li, S. Meng, L. Wang, J. Ma, *J. Org. Chem.* **2012**, *77*, 8124-8130; f) Y. Xu, S. Gsänger, M. B. Minameyer, I. Imaz, D. Maspoch, O. Shyshov, F. Schwer, X. Ribas, T. Drewello, B. Meyer, M. von Delius, *J. Am. Chem. Soc.* **2019**, *141*, 18500-18507.

[8] a) T. R. Cook, P. J. Stang, *Chem. Rev.* **2015**, *115*, 7001–7045; b) A. J. McConnell, *Chem. Soc. Rev.* **2022**, *51*, 2957–2971; c) A. Tarzia, K. E. Jelfs, *Chem. Commun.* **2022**, *58*, 3717–3730; d) D. Fujita, Y. Ueda, S. Sato, N. Mizuno, T. Kumasaka, M. Fujita, *Nature* **2016**, *540*, 563–566; e) A. Takai, T. Kajitani, T. Fukushima, K. Kishikawa, T. Yasuda, M. Takeuchi, *J. Am. Chem. Soc.* **2016**, *138*, 11245-11253; f) S. Ogi, V. Stepanenko, K. Sugiyasu, M. Takeuchi, F. Würthner, *J. Am. Chem. Soc.* **2015**, *137*, 3300-3307; g) N. Sasaki, M. F. J. Mabesoone, J. Kikkawa, T. Fukui, N. Shioya, T. Shimoaka, T. Hasegawa, H. Takagi, R. Haruki, N. Shimizu, S. Adachi, E. W. Meijer, M. Takeuchi, K. Sugiyasu, *Nat. Comm.* **2020**, *11*, 3578; h) G. M. Lang, T. Shima, L. Wang, K. J. Cluff, K. Skopek, F. Hampel, J. Blümel, J. A. Gladysz, *J. Am. Chem. Soc.* **2016**, *138*, 7649-7663; i) A. L. Estrada, L. Wang, G. Hess, F. Hampel, J. A. Gladysz, *Inorg. Chem.* **2022**, *61*, 17012-17025.

[9] a) Y. Domoto, M. Abe, K. Yamamoto, T. Kikuchi, M. Fujita, *Chem. Sci.* **2020**, *11*, 10457–10460; b) Y. Domoto, M. Abe, T. Kikuchi, M. Fujita, *Angew. Chem. Int. Ed.* **2020**, *132*, 3478–3482; c) Y. Domoto, M. Abe, M. Fujita, *J. Am. Chem. Soc.* **2021**, *143*, 8578–8582; d) Y. Domoto, K. Yamamoto, S. Horie, Z. Yu, M. Fujita, *Chem. Sci.* **2022**, *13*, 4372–4376.

[10] a) D. Wang, B. Zhang, C. He, P. Wu, C. Duan, *Chem. Commun.* **2010**, *46*, 4728; b) L. Zhang, R. Das, C. Li, Y. Wang, F. E. Hahn, K. Hua, L. Sun, Y. Han, *Angew. Chem. Int. Ed.* **2019**, *58*, 13360–13364; c) Y.-W. Zhang, S. Bai, Y.-Y. Wang, Y.-F. Han, *J. Am. Chem. Soc.* **2020**, *142*, 13614–13621.

[11] a) T. Sawada, A. Saito, K. Tamiya, K. Shimokawa, Y. Hisada, M. Fujita, *Nat. Commun.* **2019**, *10*, 921; b) Y. Inomata, T. Sawada, M. Fujita, *Chem* **2020**, *6*, 294–303; c) J. E. M. Lewis, *Chem* **2020**, *6*, 14–15; d) Y. Inomata, T. Sawada, M. Fujita, *J. Am. Chem. Soc.* **2021**, *143*, 16734–16739; e) T. Sawada, M. Fujita, *Bull. Chem. Soc. Jpn.* **2021**, *94*, 2342–2350.

[12] a) M. Bera, G. Aromi, W. T. Wong, D. Ray, *Chem. Comm.* **2006**, *6*, 671; b) S.-K. Peng, H. Yang, D. Luo, M. Xie, W.-J. Tang, G.-H. Ning, D. Li, *Inorg. Chem. Front.* **2022**, *9*, 5327–5334; c) Y. Wu, M. Xie, J.-K. Jin, Z.-Y. Zhang, H. Hu, Y.-P. Tian, Y.-Q. Xiao, G.-H. Ning, D. Li, X. Jiang, *Small Struct.* **2022**, *3*, 2100155.

[13] a) L. J. Wang, S. Bai, Y. F. Han, *J. Am. Chem. Soc.* **2022**, *144*, 16191–16198; b) A. Sarwa, A. Białońska, M. Garbicz, B. Szyszko, *Chem. Eur. J.* **2023**, *61*, e202203850.

[14] a) H. Kwon, E. Pietrasiak, T. Ohhara, A. Nakao, B. Chae, C.-C. Hwang, D. Jung, I.-C. Hwang, Y. H. Ko, K. Kim, E. Lee, *Inorg. Chem.* **2021**, *60*, 6403–6409; b) S. Horiuchi, S. Moon, A. Ito, J. Tessarolo, E. Sakuda, Y. Arikawa, G. H. Clever, K. Umakoshi, *Angew. Chem. Int. Ed.* **2021**, *60*, 10654–10660; c) M. Cuerva, R. García-Fandiño, C. Vázquez-Vázquez, M. A. López-Quintela, J. Montenegro, J. R. Granja, *ACS Nano* **2015**, *9*, 10834–10843.

[15] J. Zhang, M. Nieuwenhuyzen, J. P. H. Charmant, S. L. James, *Chem. Commun.* **2004**, 2808.

[16] J. P. Carpenter, C. T. McTernan, T. K. Ronson, J. R. Nitschke, *J. Am. Chem. Soc.* **2019**, *141*, 11409–11413.

[17] C. T. McTernan, T. K. Ronson, J. R. Nitschke, *J. Am. Chem. Soc.* **2021**, *143*, 664–670.

[18] Y. Tamura, H. Takezawa, M. Fujita, *J. Am. Chem. Soc.* **2020**, *142*, 5504–5508.

[19] **Note:** X-ray crystallographic data are available free of charge from Cambridge Crystallographic Data Centre, accession code CCDC 2215164. They can be obtained *via* www.ccdc.cam.ac.uk/data_request/cif, or by emailing data_request@ccdc.cam.ac.uk, or by contaciting The Cambridge Crystallographic Data Centre, 12 Union Road, Cambridge, CB2 1EZ, UK; fax: +44 1223 336033.

[20] T. Tsuda, S. Ohba, M. Takahashi, M. Ito, *Acta Crystallogr. Sect. C Cryst. Struct. Commun.* **1989**, *45*, 887–890.

[21] a) G.-H. Niu, H. C. Wentz, S.-L. Zheng, M. G. Campbell, *Inorg. Chem. Commun.* **2019**, *101*, 142–144; b) A. N. Desnoyer, A. Nicolay, P. Rios, M. S. Ziegler, T. D. Tilley, *Acc. Chem. Res.* **2020**, *53*, 1944–1956.

[22] J. B. Maglic, R. Lavendomme, *J. Appl. Crystallogr.* **2022**, *55*, 1033–1044.

[23] D. Brynn Hibbert, P. Thordarson, *Chem. Commun.* **2016**, *52*, 12792–12805.

[24] N. L. Allinger, Y. H. Yuh, J. H. Lii, *J. Am. Chem. Soc.* **1989**, *111*, 8551–8566.

[25] **Note**: Geometry optimized structures were modelled using the MM3 force field on SCIGRESS software (Fujitsu Limited, Tokyo, Japan, 2013) Version FJ 2.6 (EU 3.1.9) Build 5996.8255.20141202., 2013.

[26] M. Kieffer, A. M. Garcia, C. J. E. Haynes, S. Kralj, D. Iglesias, J. R. Nitschke, S. Marchesan, *Angew. Chem. Int. Ed.* **2019**, *58*, 7982–7986.

[27] D. R. Herschbach, V. W. Laurie, *J. Chem. Phys.* **1961**, *35*, 458–464.

10.1002/anie.202301612

[28] a) D. Perreault, M. Drouin, A. Michel, P. D. Harvey, *Inorg. Chem.* **1993**, *32*, 1903–1912; b) P. Harvey, *Coord. Chem. Rev.* **1996**, *153*, 175–198.
[29] K. A. Bosnick, PhD thesis, University of Toronto (Canada), **2000**.
[30] a) X. Zhao, H. Wang, B. Li, W. Zhang, X. Li, W. Zhao, C. Janiak, A. W. Heard, X. Yang, B. Wu, *Angew. Chem. Int. Ed.* **2022**, *61*, e202115042; b) M. Tang, Y. Liang, X. Lu, X. Miao, L. Jiang, J. Liu, L. Bian, S. Wang, L. Wu, Z. Liu, *Chem* **2021**, *7*, 2160–2174.
[31] M.-M. Zhang, X.-Y. Dong, Z.-Y. Wang, X.-M. Luo, J.-H. Huang, S.-Q. Zang, T. C. W. Mak, *J. Am. Chem. Soc.* **2021**, *143*, 6048–6053.

10.1002/anie.202301612

WILEY-VCH

COMMUNICATION

Entry for the Table of Contents

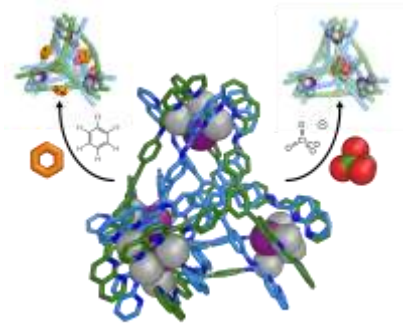

Atomically precise $[Ag_4X]^{3+}$ (X = I, Br, or Cl) clusters have been incorporated at the vertices of a double-walled tetrahedron. The cage binds guests in two distinct modes: small aromatic guests bind externally, and anionic guests bind in the central cavity. Halide ions bound to the silver clusters were observed to exchange in a well-defined hierarchy, with a preference found for the softer halides.

@ChemCambridge @SamEClark